ELSEVIER

Polymer 44 (2003) 943–952

polymer

www.elsevier.com/locate/polymer

Fluorescence studies of associative behavior of cationic surfactant moieties covalently linked to poly(acrylamide) at the surfactant head or tail

Hiromi Morimoto, Akihito Hashidzume*, Yotaro Morishima

Department of Macromolecular Science, Graduate School of Science, Osaka University, Toyonaka, Osaka 560-0043, Japan

Received 24 July 2002; received in revised form 20 November 2002; accepted 29 November 2002

Abstract

Association properties of hydrophobically modified water-soluble polymers bearing the same (or similar) hydrophobic and charged groups at different relative positions (with respect to the polymer main chain) were compared. Two types of surfactant monomers (surfmers) were synthesized; a cationic surfactant was linked to the *p*-position of styrene at the surfactant charged head (dimethyldodecyl-4-vinylbenzylammonium chloride (St-QC_{12})) or at the tail end (13-(4-vinylphenyl)tridecyltrimethylammonium bromide (St-$C_{13}Q$)). These surfmers were copolymerized with acrylamide (AAm), and the association behavior of the copolymers in water was characterized using different fluorescence techniques. The surfmer contents in the AAm/St-QC_{12} and AAm/St-$C_{13}Q$ copolymers were fixed to more or less 10 mol%. The surfmer units in the copolymers self-associate to form multipolymer aggregates. An apparent critical micelle concentration (cmc) (i.e. a polymer concentration for the onset of interpolymer association of the surfmer units) estimated from excitation spectra of pyrene probes for AAm/St-QC_{12} (cmc $= 2.6 \times 10^{-4}$ g/l) was several times lower than that for AAm/St-$C_{13}Q$ (cmc $= 1.3 \times 10^{-3}$ g/l), surfmer units in AAm/St-QC_{12} showing a stronger tendency for interpolymer association than those in AAm/St-$C_{13}Q$. The presence of excimer emissions in steady-state fluorescence spectra for the *p*-substituted styrene residues (phenylene groups) in AAm/St-$C_{13}Q$ indicated that the benzene rings are in close proximity to one another in the polymer aggregates. Steady-state fluorescence spectra and fluorescence quenching by thallium nitrate and 1-nitrohexane indicated that the phenylene groups in AAm/St-$C_{13}Q$ were incorporated in hydrophobic microdomains formed from surfactant hydrocarbon chains, whereas the phenylene groups in AAm/St-QC_{12} are located near the surface of polymer aggregates in a way that they are sufficiently apart from each other and hence no excimer is formed.

Keywords: Poly(acrylamide); Surfmer; Fluorescence techniques

1. Introduction

Recent years have brought considerable interest in studying hydrophobically modified water-soluble polymers because of their relevance to biological macromolecular systems and also because of their potential in commercial applications such as water-borne paint and coating fluids, cosmetics and personal care goods, drug delivery systems, and water treatment [1–3]. A large number of investigations have focused on ionic and nonionic water-soluble polymers modified with various hydrophobes.

Hydrophobic self-associations in these amphiphilic polymers are induced in water within the same polymer chain or between different chains depending on macromolecular architecture. It has been well-established that the types of hydrophilic [4–12] and hydrophobic [13–19] monomer units, copolymer composition [13,14,19–24], sequence distribution of hydrophilic and hydrophobic monomer units along the polymer chain [21], and spacer between the hydrophobe and polymer backbone [19,25–30] are some of the important architectural parameters for the self-associative properties of amphiphilic random copolymers.

In the case of amphiphilic polymers where ionic amphiphiles are covalently linked to nonionic water-soluble polymers, the relative positions of the charge and hydrophobe with respect to the polymer main chain seem to be an important parameter to influence the properties of the polymer. Several types of homo- and copolymers of

---

[*] Corresponding author. Tel.: +81-6-6850-5462; fax: +81-6-6850-5461.
E-mail address: akihito@chem.sci.osaka-u.ac.jp (A. Hashidzume).

0032-3861/03/$ - see front matter © 2002 Elsevier Science Ltd. All rights reserved.
PII: S0032-3861(02)00897-2

'surfactant monomers' or 'surfmers' have been reported [31–36]. There seems to be a trend that polymers with surfactant fragments bound to the main chain at the surfactant tail end are soluble in water while those with surfactant fragments bound at the surfactant head are insoluble [37–43]. These observations reported in the literature prompted us to systematically compare self-associative properties of amphiphilic polymers possessing a surfactant moiety attached to the polymer main chain at different relative positions of the charge and hydrophobe (Fig. 1). To synthesize such polymers, we chose a set of cationic surfmers in which the relative positions of a polymerizable group and a charged group are different. Since we intended to compare association properties in aqueous solutions, we employed random copolymers of acrylamide (AAm) and the surfmers to ensure water solubility.

Copolymers of AAm and various surfmers have been prepared, and their self-association properties in aqueous media have been studied by McCormick et al. [15,21,44] and Candau et al. [45–48]. Surfactant-carrying poly(acrylamide)s (poly(AAm)s) with surfmer contents lower than 5 mol% have been prepared by micellar copolymerization in aqueous media, which leads to the formation of multiblocky sequences [15,44–47]. The present work compares association characteristics of a cationic surfactant covalently bound to poly(AAm) at the surfactant head or at the tail end. Polymers synthesized in the present study are copolymers of AAm and either of the two types of styrene-based cationic surfmers where a cationic surfactant was linked at the *p*-position of styrene with the surfactant charged head (St-QC_{12}) or with the tail end (St-$C_{13}Q$). The contents of the surfmers in the copolymers are fixed to ca. 10 mol%. Sequence distributions of these copolymers are statistical because the copolymerization was performed in homogeneous solutions using *N*,*N*-dimethylformamide as solvent. Various fluorescence techniques were employed to characterize their self-association behavior in water.

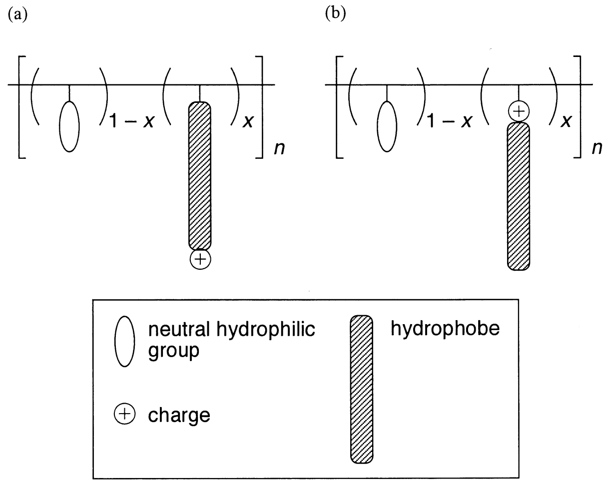

Fig. 1. Schematic illustration of nonionic water-soluble polymers tethered with a surfactant moiety at its tail end (a) or at its charged head (b).

2. Experimental

2.1. Materials

4-Vinylbenzylchloride (Aldrich), 1,12-dibromododecane (Aldrich), *N*,*N*-dimethyldodecylamine (Wako), and lithium tetrachlorocuprate(II) (Li_2CuCl_4) (0.1 M tetrahydrofuran (THF) solution) (Aldrich) were used without purification. Acrylamide (AAm) (Wako) was recrystallized from ethyl acetate. 2,2′-Azobis(isobutyronitrile) (AIBN) (Wako) was recrystallized from methanol. Diethyl ether, THF, and toluene were refluxed over sodium in the presence of benzophenone and distilled under an argon atmosphere. *N*,*N*-Dimethylformamide (DMF) was purified by distillation under reduced pressure. Milli-Q water was used to prepare polymer solutions. Pyrene was recrystallized twice from ethanol. Analytical grade NaCl, thallium nitrate, and 1-nitrohexane were used without further purification.

2.2. Preparation of surfmers

2.2.1. 13-(4-Vinylphenyl)tridecyltrimethylammonium bromide (St-$C_{13}Q$)

St-$C_{13}Q$ was synthesized according to the synthesis of 5-(4-vinylphenyl)pentyltrimethylammonium bromide [49] with slight modification as follows: To a stirred suspension of magnesium flakes (2.0 g, 0.082 mol) in diethyl ether (10 ml) was added 4-vinylbenzylchloride (6.2 g, 0.040 mol) in 10 ml of diethyl ether dropwise at 0 °C for 30 min under an argon atmosphere. After 3 h, the reaction mixture (Grignard reagent) was allowed to stand for 10 min and the supernatant was transferred into a dropping funnel. The solution of the Grignard reagent in diethyl ether was added dropwise over a period of 1 h to a mixture of 40 ml THF solution of 1,12-dibromododecane (13.1 g, 0.040 mol) containing 3.5 ml of a 0.1 M Li_2CuCl_4 in THF at 10 °C. The reaction mixture was stirred at 30 °C for additional 3 h under an argon atmosphere. After removal of the solvent under vacuum, 2N HCl (20 ml) and diethyl ether (100 ml) were added to the residue. The organic phase was washed with saturated $NaHCO_3$ (10 ml) and saturated NaCl (10 ml), and dried over anhydrous Na_2SO_4. After evaporation of diethyl ether, a yellow liquid was obtained. After extraction from the yellow liquid with ethanol, crude 4-(13-bromotridecyl)styrene containing ca. 10% of 1,14-bis(4-vinylphenyl)tetradecane as an impurity was obtained as a colorless powder from an ethanol-soluble fraction; yield 1.1 g, 7.5%.

The crude 4-(13-bromotridecyl)styrene (1.1 g, 2.7 mmol) was dissolved in toluene (10 ml). Trimethylamine gas, which was distilled from a 30 wt% aqueous solution (16 ml), was bubbled into the toluene solution at 0 °C. The reaction mixture was kept at 30 °C with stirring for 4 days. After removal of the solvent and excess trimethylamine under reduced pressure, a white residue was obtained. The residue was washed with *n*-hexane to remove unreacted 4-(13-bromotridecyl)styrene and 1,14-bis(4-vinylphenyl)tetradecane. After drying under reduced pressure, St-C_{13}Q was obtained as a colorless powder; yield 0.26 g, 11% based on 4-(13-bromotridecyl)styrene; mp 158–159 °C; ^{1}H NMR (CD_3Cl, 270 Hz): δ 1.2–1.5 (20H, CH_2), 1.7–1.8 (2H, m, CH_2), 2.59 (2H, t, $J = 7.6$ Hz), 3.47 (9H, s, $(CH_3)_3N^+$), 3.56 (2H, m, CH_2N^+), 5.18 (1H, dd, $J = 10.9$, 1.0 Hz, *trans*-CH=), 5.69 (1H, dd, $J = 17.5$, 1.0 Hz, *cis*-CH=), 6.69 (1H, dd, $J = 17.5$, 10.9 Hz, CH=), 7.13 (2H, d, $J = 7.9$ Hz, phenyl), 7.32 (2H, d, $J = 7.9$ Hz, phenyl). Anal. Calcd for $C_{24}H_{42}NBr(H_2O)_{0.5}$: C, 66.49; H, 10.00; N, 3.23. Found: C, 66.50; H, 10.00; N, 3.31.

2.2.2. Dimethyldodecyl-4-vinylbenzylammonium chloride (St-QC_{12})

St-QC_{12} was prepared according to the procedure of Cochin et al. [45]. In a 200 ml flask, 4-vinylbenzyl chloride (6.7 ml, 0.047 mol) was mixed with *N,N*-dimethyldodecylamine (11.7 g, 0.055 mol) and a small quantity of 2,6-di-*t*-butyl-*p*-cresol. This reaction mixture was maintained at 30 °C for 17 h, and then colorless precipitate was formed. The product was washed with diethyl ether several times and dried under vacuum at room temperature. St-QC_{12} was purified by recrystallization from acetone/diethyl ether (10/1, v/v); yield 9.5 g, 55%; mp 69.9–70.1 °C; ^{1}H NMR (CD_3Cl, 270 Hz): δ 0.87 (3H, t, $J = 6.6$ Hz, CH_3), 1.2–1.4 (20H, CH_2), 3.29 (6H, s, $(CH_3)_2N^+$), 3.48 (2H, m, CH_2N^+), 5.05 (2H, s, CH_2N^+), 5.35 (1H, d, $J = 11.2$ Hz, *trans*-CH=), 5.80 (1H, d, $J = 17.2$ Hz, *cis*-CH=), 6.65 (1H, dd, $J = 11.2$, 17.2 Hz, CH=), 7.43 (2H, d, $J = 7.9$ Hz, phenyl), 7.60 (2H, d, $J = 7.9$ Hz, phenyl). Anal. Calcd for $C_{23}H_{40}NCl(H_2O)_{0.7}$: C, 72.96; H, 11.02; N, 3.70. Found: C, 72.87; H, 11.05, N, 3.79.

2.3. Copolymerization

Copolymers of AAm with St-C_{13}Q and with St-QC_{12} were prepared by free radical polymerization initiated by AIBN in DMF. A representative procedure for the copolymerization is as follows: AAm, St-C_{13}Q or St-QC_{12}, and 0.1 mol% (based on the total monomers) of AIBN were dissolved in DMF in a glass ampule. The ampule was outgassed by six freeze-pump-thaw cycles on a high vacuum line. The sealed ampule was immersed in a water bath thermostatted at 60 °C for 16 h. After cooling the reaction mixture, the copolymer recovered by filtration was washed with methanol repeatedly, and then purified by dialysis against deionized water for 1 week. Compositions of the copolymers were determined by ^{1}H NMR.

2.4. Measurements

2.4.1. ^{1}H NMR

^{1}H NMR spectra for surfmers and copolymers were measured with a JEOL JNM EX270 NMR spectrometer in $CDCl_3$ or D_2O at 30 °C.

2.4.2. Viscosity

Viscosities were measured with an Ubbelohde type viscometer at 30 °C using formamide as solvent. Each sample solution was filtered with a 0.45 μm membrane filter.

2.4.3. Fluorescence

Steady-state fluorescence spectra were recorded on a Hitachi F-4500 fluorescence spectrophotometer. The slit widths for both the excitation and emission sides were kept at 2.5 nm.

2.4.3.1. Measurements of fluorescence spectra of molecular pyrene solubilized by polymers in water. Excitation spectra of pyrene were monitored at 372 nm. Sample solutions were prepared by dissolving a known amount of polymer in pyrene-saturated water. For determination of the critical micelle concentration (cmc) of the polymers, excitation spectra of pyrene were obtained at varying concentrations of the polymers, following the procedures reported by Wilhelm et al. [50].

2.4.3.2. Measurements of fluorescence spectra of pyrene-free aqueous solutions of the polymers. Emission spectra of copolymers were measured with excitation at 260 nm.

2.4.4. Fluorescence quenching

Aliquots of a stock solution of quencher (thallium nitrate or 1-nitrohexane) were added to aqueous solutions of the copolymers with quencher concentrations ranging 0–5 mM. Fluorescence spectra were measured with excitation at 260 nm.

2.4.5. Quasielastic light scattering (QELS)

The distribution of the relaxation times and the apparent hydrodynamic radius (R_h) were measured with an Otsuka Electronics Photal DLS-7000 light scattering spectrometer equipped with an argon ion laser (output power = 50 mW at $\lambda = 488$ nm) and an ALV-5000 multi-τ-digital time correlator. All measurements were performed at 25 °C. The distributions of relaxation times and R_h for polymer aggregates were measured varying the scattering angles. Sample solutions were filtered prior to measurement using a 0.80 μm pore size disposable membrane filter. To obtain the relaxation time distribution, the inverse Laplace transform analysis was performed by conforming the

REPES algorithm [51,52]:

$$g^{(1)}(t) = \int \tau A(\tau)\exp(-t/\tau)dln\tau \qquad (1)$$

where, τ is the relaxation time and $g^{(1)}(t)$ is the normalized autocorrelation function. Apparent values of R_h were calculated using the Einstein–Stokes relation, $R_h = k_BT/(6\pi\eta D)$, where k_B is Boltzman's constant, T is the absolute temperature, η is the solvent viscosity, and D is the diffusion coefficient determined by QELS.

3. Results and discussion

3.1. Basic characteristics of the copolymers

Copolymers of AAm and styrene-based cationic surfmers prepared in this study are presented in Scheme 1 (AAm/St-C_{13}Q and AAm/St-QC_{12}). In AAm/St-QC_{12}, a surfactant moiety is linked to the styrene residue at the surfactant head while in AAm/St-C_{13}Q, a surfactant of a similar structure is linked at the surfactant tail end. The contents of the surfmers in the copolymers were fixed to ca. 10 mol% (Table 1). In contrast to the case of micellar polymerization reported for the synthesis of hydrophobically modified poly(AAm)s [21,53], a homogeneous solution polymerization technique employed in the present study yields copolymers with a statistical distribution of the surfactant units.

Fig. 2 shows reduced viscosity for AAm/St-C_{13}Q and AAm/St-QC_{12} in formamide as a function of polymer concentration (C_p). Viscosity-average molecular weights (M_v's) for AAm/St-C_{13}Q and AAm/St-QC_{12} were roughly estimated to be 1.10×10^5 and 1.90×10^5, respectively from the intrinsic viscosities ([η]) using the relationship $[\eta] = 1.08 \times 10^{-3} M_v^{0.54}$ established for poly(AAm) in formamide at 30 °C [54].

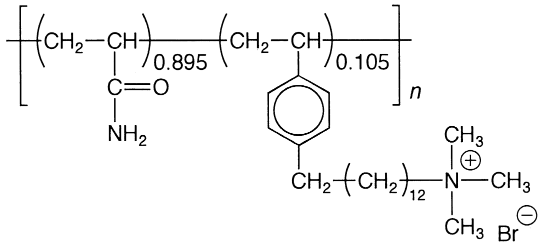

AAm/St-C_{13}Q

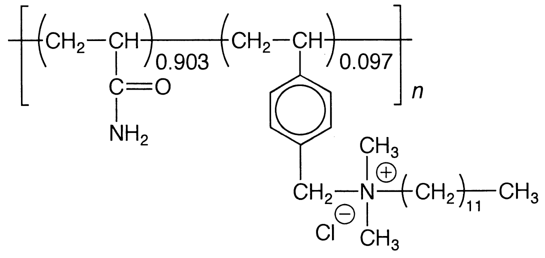

AAm/St-QC_{12}

Scheme 1. Copolymer Structures for AAm/St-C_{13}Q and AAm/St-QC_{12}.

Table 1
Characteristics of the copolymers

Copolymer	f_s[a] (mol%)	Yield (%)	[η][b] (dL/g)	M_v ($\times 10^{-4}$)[c]
AAm/St-C_{13}Q	10.5	20	0.57	11.0
AAm/St-QC_{12}	9.7	57	0.78	19.0

[a] Mole percent content of the surfmer in the copolymer determined by ^{1}H NMR in D_2O.

[b] Measured in formamide at 30 °C.

[c] Calculated using the relationship $[\eta] = 1.08 \times 10^{-3} M_v^{0.54}$ established for poly(AAm) in formamide at 30 °C [54].

3.2. Apparent critical micelle concentration

Excitation spectra for pyrene probes solubilized in aqueous solutions of AAm/St-C_{13}Q and AAm/St-QC_{12} of varying C_p are shown in Fig. 3. The spectra show peaks associated with the pyrene (0,0) band at 333 nm in a low C_p region, the peak shifting to 338 nm in a high C_p region. The transition of the peak from 333 to 338 nm occurs in a narrow range of C_p. It is known that the (0,0) absorption maximum of pyrene in water at 333 nm shifts to a longer wavelength when pyrene is solubilized in hydrophobic phases [50]. Thus, we estimated the ratio of the intensity at 338 nm to that at 333 nm (I_{338}/I_{333}) and plotted in Fig. 4 as a function of C_p for AAm/St-C_{13}Q and AAm/St-QC_{12}. In the low C_p regime ($< 10^{-3}$ g/l), the I_{338}/I_{333} ratio is practically independent of C_p but the ratio starts to increase significantly as C_p is increased to a certain level. This observation is indicative of the presence of interpolymer association that starts to occur when C_p is increased to a certain level. The ratio of the third and the first vibronic peaks in steady-state emission spectra of pyrene probes as a function of C_p exhibited the same tendency (not shown). In addition, the maximum of I_{338}/I_{333} for AAm/St-QC_{12} (≈ 1.53) is slightly larger than that of AAm/St-C_{13}Q (≈ 1.45). This observation may be due to the difference in the band width of the 338 nm absorption for both the copolymers. As shown in Fig. 3, the peak at 338 nm for

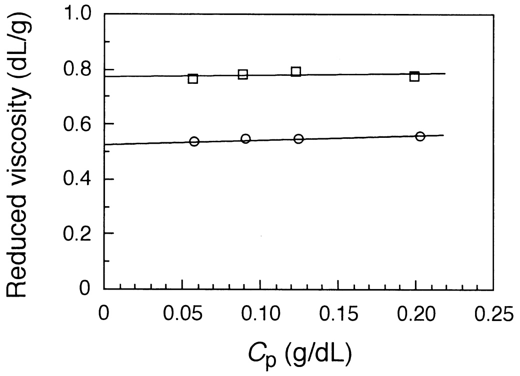

Fig. 2. Plots of reduced viscosity against C_p for AAm/St-C_{13}Q (○) and AAm/St-QC_{12} (□) in formamide.

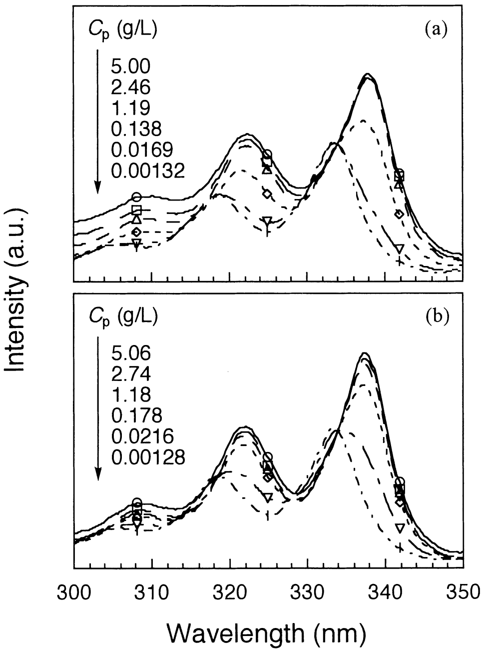

Fig. 3. Steady-state fluorescence excitation spectra monitored at 372 nm for pyrene probes in 0.02 M NaCl in the presence of varying concentrations of AAm/St-$C_{13}Q$ (a) and AAm/St-QC_{12} (b). Pyrene concentration was fixed to 4.0×10^{-7} M.

AAm/St-$C_{13}Q$ is slightly broader than that for AAm/St-QC_{12}, suggesting that hydrophobic microdomains in aggregates of the former copolymer is somewhat heterogeneous compared to those of the latter.

On the basis of the data presented in Fig. 4, the ratio of the pyrene concentrations in the hydrophobic phase and in the aqueous phase ($[Py]_m/[Py]_w$) was calculated by assuming the minimum and maximum values of I_{338}/I_{333} at low and high C_p, respectively and plotted in Fig. 5 against C_p for AAm/St-$C_{13}Q$ and AAm/St-QC_{12}. The plots show a break in a low C_p region (inset in Fig. 5) which corresponds to the onset of interpolymer associations of the surfmer units, and therefore the onset concentration may be viewed as an apparent cmc for the polymer-bound surfactant moieties. From the break observed in the $[Py]_m/[Py]_w$ vs. C_p plot, apparent values of cmc were estimated to be 1.3×10^{-3} and 2.6×10^{-4} g/l for AAm/St-$C_{13}Q$ and AAm/St-QC_{12}, respectively. These apparent cmc values correspond to 1.3×10^{-3} and 2.5×10^{-4} mM surfmer units for AAm/St-$C_{13}Q$ and AAm/St-QC_{12}, respectively. These cmc values in unit molar concentrations are more than 1 order of magnitude lower than that for dodecyltrimethylammonium bromide (DTAB) (ca. 15 mM) [55], the polymer chain inducing the formation of a micelle-like structure at much lower concentrations of the surfactant residues. Apparent cmc for AAm/St-QC_{12} is several times lower than that for AAm/St-$C_{13}Q$. This observation indicates that cationic surfactants in AAm/St-QC_{12} have a stronger tendency for interpolymer association than those in AAm/St-$C_{13}Q$.

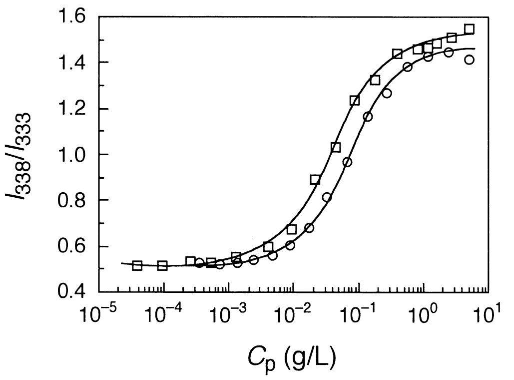

Fig. 4. Plots of I_{338}/I_{333} against C_p for AAm/St-$C_{13}Q$ (○) and AAm/St-QC_{12} (□) in 0.02 M NaCl.

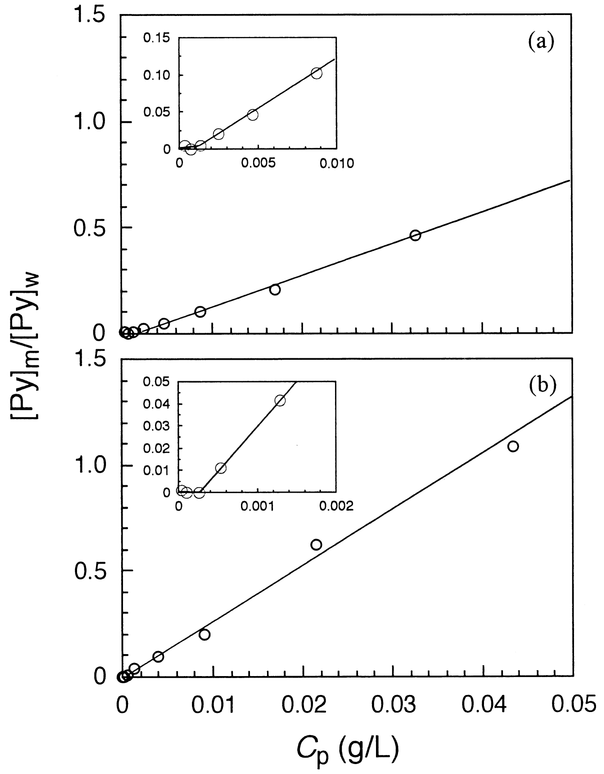

Fig. 5. Plots of $[Py]_m/[Py]_w$ estimated from I_{338}/I_{333} against C_p for AAm/St-$C_{13}Q$ (a) and AAm/St-QC_{12} (b) in 0.02 M NaCl. The insets show plots for low C_p regions on expanded scales.

3.3. Steady-state fluorescence spectra for the polymer-bound phenylene moieties

The phenylene residues in the two copolymers were found to be weakly fluorescent. Steady-state fluorescence spectra for AAm/St-$C_{13}Q$ and AAm/St-QC_{12} in aqueous solutions are quite different, as compared in Fig. 6. The fluorescence intensity for AAm/St-$C_{13}Q$ is nearly three times stronger than that for AAm/St-QC_{12} at nearly the same concentrations of phenylene moieties (ca. 0.98 mM). The spectrum for AAm/St-$C_{13}Q$ shows two peaks with maxima at ca. 290 and 300 nm. As will be discussed later, the peak at the longer wavelength is assigned to an excimer

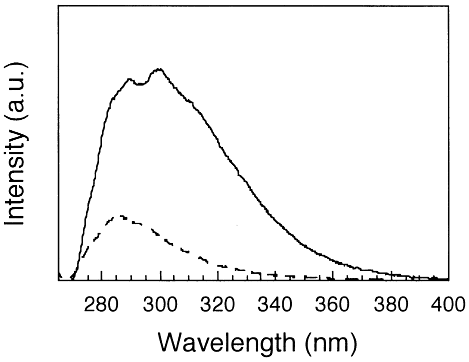

Fig. 6. Steady-state fluorescence spectra for AAm/St-C_{13}Q (solid line) and AAm/St-QC_{12} (broken line) at $C_p = 1.0$ g/l in 0.02 M NaCl. Excitation wavelength was 260 nm.

emission of the phenylene residues in polymer aggregates of AAm/St-C_{13}Q. On the other hand, AAm/St-QC_{12} exhibits a peak with a maximum around 285 nm. These differences in the fluorescence spectra are attributed to a difference in the type of aggregates of the two copolymers, as will be discussed in detail in a later subsection.

Fig. 7 compares fluorescence spectra for AAm/St-C_{13}Q and AAm/St-QC_{12} (normalized at 290 and 285 nm, respectively) at varying C_p in aqueous solutions without added NaCl. In the case of AAm/St-C_{13}Q, the intensity of fluorescence around 300 nm relative to that at 290 nm increases with increasing C_p, suggesting that the emission is due to an excimer of phenylene moieties [56,57]; the phenylene residues are in close proximity to each other in polymer aggregates and the fraction of the phenylene residues forming the excimer increases with C_p. The band profiles in absorption spectra for AAm/St-C_{13}Q at different C_p were almost the same, suggesting that the excimer emission is not due to ground-state dimers. The polymer main chain may disturb the formation of ground-state dimer of phynylene groups. On the other hand, in the case of AAm/St-QC_{12}, the shoulder around 295 nm increases only slightly with increasing C_p, suggesting that the excimer formation is prohibited by electrostatic repulsion between trimethylammonium groups closely attached to the phenylene group.

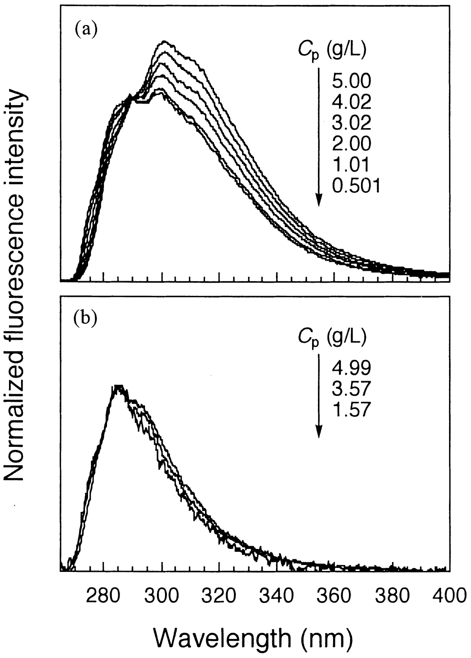

Fig. 7. Steady-state fluorescence spectra for AAm/St-C_{13}Q (a) and AAm/St-QC_{12} (b) at varying C_p without added NaCl. Excitation wavelength was 260 nm.

3.4. Fluorescence quenching for the polymer-bound phenylene residues by thallium nitrate and 1-nitrohexane

To obtain information about microenvironments around the phenylene residues in the two copolymers, fluorescence quenching for the phenylene moieties was investigated. When a bimolecular fluorescence quenching due to a diffusional encounter of a fluorophore and a quencher competes with the unimolecular decay of a singlet-excited state of the fluorophore, the fluorescence quenching is dynamic and follows the Stern–Volmer kinetics [58]:

$$I/I_0 = 1 + K[\mathrm{Q}] \qquad (2)$$

where I and I_0 are the fluorescence intensity in the presence and absence of the quencher, respectively, K is the Stern–Volmer constant for the accessible chromophores, and [Q] is the quencher concentration. On the other hand, when the quenching occurs between a fluorophore and a quencher at their fixed sites without diffusional collision (or the diffusion of a quencher to encounter with a fluorophore is much slower than the unperturbed decay of the fluorophore), the fluorescence quenching is static in nature and may follow the Perrin model [59] which assumes an active sphere about the fluorophore:

$$\ln(I/I_0) = n = [\mathrm{Q}]/[\mathrm{A}] \qquad (3)$$

where n is the number of quencher in an active sphere and [A] is the concentration of active sphere. The active sphere is a volume where a quencher present within this volume quenches the fluorophore with unity efficiency while quenchers outside the volume do not.

In this work, thallium nitrate (a cationic quencher) and 1-nitrohexane (a hydrophobic quencher) were used as quencher. Since Tl^+ ions exist in the aqueous phase and quench fluorescence of aromatic fluorophores through a short range interaction due to an external heavy atom effect [60], fluorescence of phenylene residues exposed to the aqueous phase may be favorably quenched by Tl^+ ions. On the other hand, since 1-nitrohexane molecules exist preferentially in hydrophobic microdomains and quench fluorescence of aromatic fluorophores presumably through an electron transfer mechanism [61], fluorescence of phenylene residues incorporated in hydrophobic microdomains may be preferentially quenched by 1-nitrohexane.

Fig. 8 compares Stern–Volmer plots for AAm/St-C_{13}Q

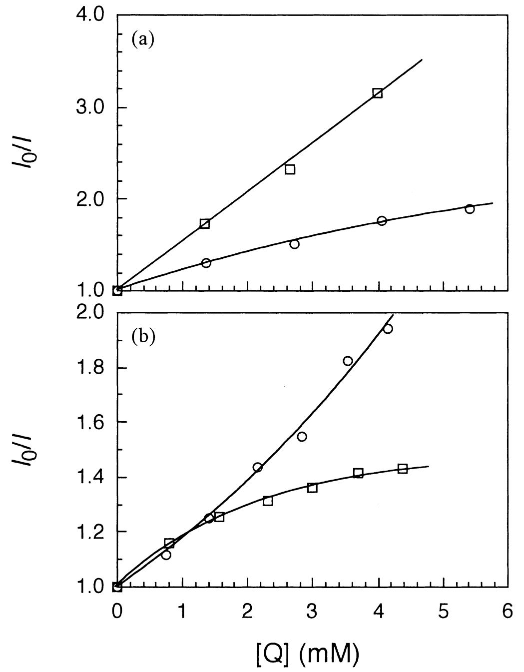

Fig. 8. Stern–Volmer plots for fluorescence quenching for AAm/St-$C_{13}Q$ (○) and AAm/St-QC_{12} (□) using thallium nitrate in 0.02 M sodium acetate (a) and 1-nitrohexane in 0.02 M NaCl (b). C_p's were fixed to 1.0 and 5.0 g/l using thallium nitrate (a) and 1-nitrohexane (b), respectively.

and AAm/St-QC_{12} using these two quenchers. Fluorescence intensity was determined from the area intensity of the emission band in the range 270–350 nm. With Tl^+ ions (Fig. 8(a)), the Stern–Volmer plot for AAm/St-QC_{12} exhibits a linear relationship, indicative of a dynamic quenching mechanism. This finding suggests that the phenylene residues in AAm/St-QC_{12} are located near the surface of polymer aggregates and hence can encounter with the cationic quencher. On the other hand, the quenching for AAm/St-$C_{13}Q$ is less effective, the plot showing a downward curvature. This observation suggests that a significant fraction of phenylene residues is not accessible to Tl^+ ions. In general, if there are two fluorophore sites, one is accessible to quenchers and the other is not, the Stern–Volmer equation (Eq. (2)) can be modified as [60]

$$I_0/(I_0 - I) = 1/\phi K[Q] + (1/\phi) \quad (4)$$

where ϕ is the fraction of the accessible chromophores. In the case of the AAm/St-$C_{13}Q$/thallium nitrate system, $I_0/(I_0 - I)$ vs. 1/[Q] plot exhibits a linear relationship (Fig. 9). From the plot, a value of $1 - \phi$ was determined to be 0.29. Since Tl^+ ions exist in the aqueous phase, the $1 - \phi$ value of 0.29 for AAm/St-$C_{13}Q$ (i.e. 29% fluorophores are not accessible to Tl^+ ions) indicates that a significant fraction of the phenylene residues in AAm/St-$C_{13}Q$ are protected in hydrophobic microdomains from the access of Tl^+ ions.

With 1-nitrohexane (Fig. 8(b)), the Stern–Volmer plot for AAm/St-QC_{12} shows a downward curvature, indicative of a significant fraction of the phenylene residues not accessible to 1-nitrohexane. The quenching data for AAm/St-QC_{12} in Fig. 8(b) followed Eq. (4) giving a linear relationship (Fig. 9). From the plot, a value of $1 - \phi$ was determined to be 0.59 (i.e. 59% fluorophores are not accessible to 1-nitrohexane). This finding suggests that a considerable fraction of the phenylene residues in AAm/St-QC_{12} are kept from access to 1-nitrohexane because the phenylene residues are located near the surface of hydrophobic microdomain as suggested from the dynamic quenching with Tl^+ ions (Fig. 8(a)). In contrast, the plot for AAm/St-$C_{13}Q$ displays an upward curvature (Fig. 8(b)), suggesting a contribution of a static mechanism to fluorescence quenching. Thus, we applied the Perrin equation (Eq. (3)) [60] to the data for AAm/St-$C_{13}Q$ in Fig. 8(b). As can be seen in Fig. 10, the plot exhibits a linear relationship passing through the origin, indicative of a static quenching mechanism. This observation suggests that the phenylene residues in AAm/St-$C_{13}Q$ are incorporated in hydrophobic microdomains where 1-nitrohexane molecules are solubilized.

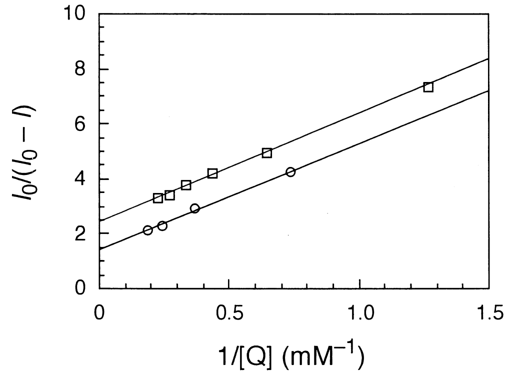

Fig. 9. Modified Stern–Volmer plots for fluorescence quenching for 1.0 g/l AAm/St-$C_{13}Q$ by thallium nitrate in 0.02 M sodium acetate (○) and 5.0 g/l AAm/St-QC_{12} by 1-nitrohexane in 0.02 M NaCl (□).

3.5. Hydrodynamic size of polymer aggregates

Fig. 11 compares relaxation time distributions in QELS measured at a scattering angle of 90° at $C_p = 5.0$ g/l in 0.02 M NaCl. AAm/St-$C_{13}Q$ exhibits a unimodal distri-

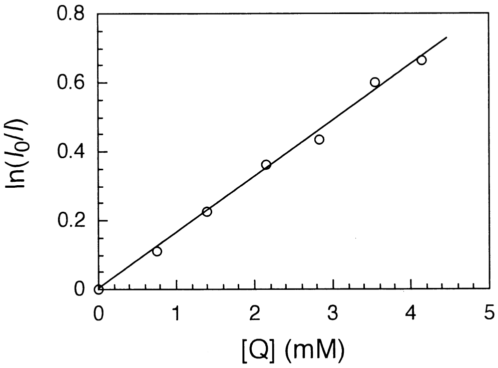

Fig. 10. Perrin plot for fluorescence quenching of 5.0 g/l AAm/St-$C_{13}Q$ by 1-nitrohexane in 0.02 M NaCl.

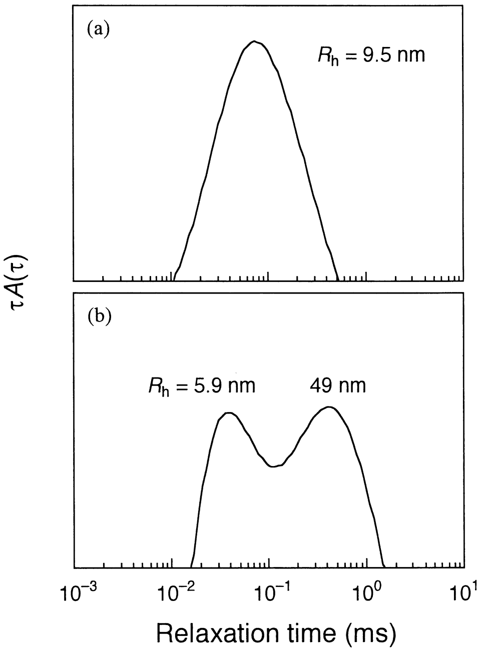

Fig. 11. Relaxation time distributions in QELS for AAm/St-$C_{13}Q$ (a) and AAm/St-QC_{12} (b) measured at $\theta = 90°$ at $C_p = 5.0$ g/l in 0.02 M NaCl.

bution with a peak corresponding to $R_h = 9.5$ nm due to polymer aggregates of a small number of polymer chains. On the other hand, AAm/St-QC_{12} exhibits a bimodal distribution at the same C_p with peaks corresponding to $R_h = 5.9$ and 49 nm. These data also indicate that cationic surfactant moieties in AAm/St-QC_{12} show a stronger tendency for interpolymer association than those in AAm/St-$C_{13}Q$, consistent with the apparent cmc values for these copolymers.

3.6. Association models for AAm/St-$C_{13}Q$ and AAm/St-QC_{12}

Based on the characterization data described above, we propose association models for AAm/St-$C_{13}Q$ and AAm/St-QC_{12}, as conceptually illustrated in Fig. 12. In the case of AAm/St-$C_{13}Q$ in which cationic surfactants are covalently bound to the main chain at the hydrophobic tail end, electrostatic repulsion between different polymer chains may disturb interpolymer association, resulting in a weaker tendency for interpolymer aggregation. Since the phenylene residue in AAm/St-$C_{13}Q$ is distant from the positive charge, the phenylene moieties may be readily incorporated in hydrophobic microdomains formed from the long alkyl chains. However, hydrophobic microdomains of AAm/St-$C_{13}Q$ may be looser than that of low molecular weight cationic surfactants, such as DTAB, because of the excluded volume effect of the hydrophilic polymer main chain. On the other hand, since AAm/St-QC_{12} has cationic surfactants covalently bound to the main chain at the charged head, their hydrophobic tails are apart from the main chain, leading to a favorable situation for interpolymer associations. Since the phenylene residue in AAm/St-QC_{12} is linked to the quaternary ammonium group, the phenylene moieties may be located near the surface of polymer aggregates, as suggested by fluorescence quenching. The present study confirms that cationic surfactants covalently-bound to poly(AAm) of similar molecular weights, similar sequence distributions, and similar contents of surfmers show different association behavior in aqueous media, when surfactant fragments are linked to the polymer backbone at the charged head or hydrophobic tail end; the relative positions of the charge and hydrophobe with respect to the polymer main chain are an important structural factor determining association properties.

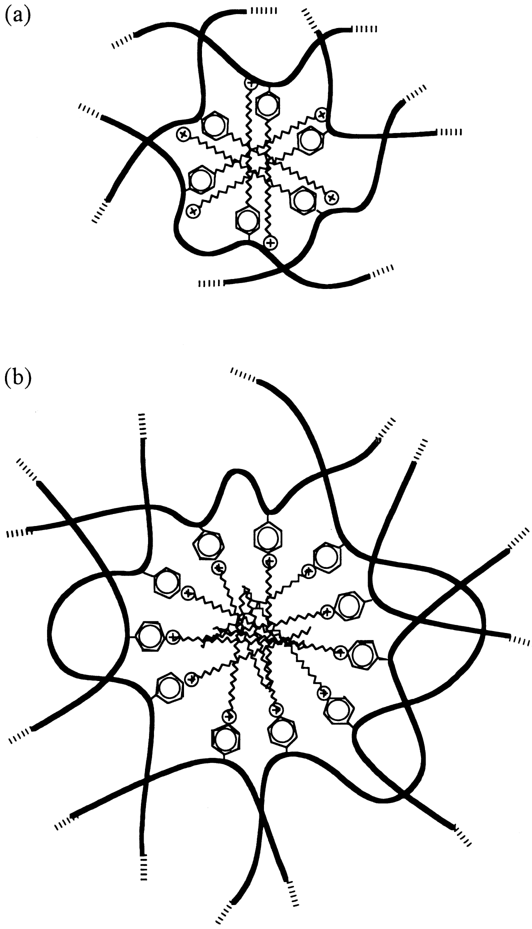

Fig. 12. Conceptual illustration of association models for AAm/St-$C_{13}Q$ (a) and AAm/St-QC_{12} (b).

4. Conclusion

The self-association properties in water of the copolymers of AAm and two types of styrene-based cationic surfmers were characterized focusing on the effects of the relative positions of the charged and hydrophobic groups with respect to the polymer main chain on the association properties. In the surfmers used, a cationic surfactant moiety is linked to the *p*-position of styrene; in one surfmer, at the charged head (St-QC_{12}) and in the other, at the tail end (St-$C_{13}Q$). The surfmer contents in the AAm/St-QC_{12} and AAm/St-$C_{13}Q$ copolymers were fixed to more or less 10 mol%. Based on the excitation spectra of pyrene probes solubilized in aqueous solutions of the copolymers, apparent values of cmc (i.e. the onset concentration for interpolymer hydrophobic associations) were estimated to be 1.3×10^{-3} and 2.6×10^{-4} g/l for AAm/St-$C_{13}Q$ and AAm/St-QC_{12}, respectively. Relaxation time distributions obtained from QELS were unimodal for AAm/St-$C_{13}Q$ and bimodal for AAm/St-QC_{12}. In the bimodal distribution for AAm/St-QC_{12}, slow mode peaks due to interpolymer aggregates with $R_h = 49$ nm were observed. These data indicated that cationic surfactant moieties in AAm/St-QC_{12} showed a stronger tendency for interpolymer association than those in AAm/St-$C_{13}Q$. The observation of an excimer emission in the steady-state fluorescence spectra for AAm/St-$C_{13}Q$ revealed that the phenylene moieties were in close proximity to one another in polymer aggregates. Fluorescence quenching data using thallium nitrate and 1-nitrohexane indicated that the phenylene moieties of AAm/St-$C_{13}Q$ were incorporated in hydrophobic microdomains formed from surfactant alkyl chains. On the other hand, in the case of AAm/St-QC_{12}, steady-state fluorescence and fluorescence quenching data indicated that the phenylene residues were located near the surface of hydrophobic microdomains and that the phenylene residues are apart from one another not to form excimer. These observations indicate that the positions of the charge and hydrophobe relative to the polymer main chain are an important factor determining association properties.

Acknowledgements

This work was supported in part by Shorai Foundation for Science and Technology.

References

[1] Bock J, Varadaraj R, Schulz DN, Maurer JJ. In: Dubin PL, Bock J, Davies RM, Schulz DN, Thies C, editors. Macromolecular complexes in chemistry and biology. Berlin: Springer; 1994. p. 33–50.

[2] Glass JE, editor. Hydrophilic polymers. Performance with environmental acceptability. Advances in Chemistry Series 248, Washington, DC: American Chemical Society; 1996.

[3] McCormick CL, Armentrout RS, Cannon GC, Martin GG. In: Morishima Y, Norisuye T, Tashiro K, editors. Molecular interactions and time-space organization in macromolecular systems. Berlin: Springer; 1999. p. 125–39.

[4] McCormick CL, Middleton JC, Cummins DF. Macromolecules 1992; 25:1201–6.

[5] McCormick CL, Elliott DL. Macromolecules 1986;19:542–7.

[6] Kathmann EE, White LA, McCormick CL. Macromolecules 1996;29: 5273–8.

[7] Newman JK, McCormick CL. Macromolecules 1994;27:5114–22.

[8] Neidlinger HH, Chen GS, McCormick CL. J Appl Polym Sci 1984;29: 713–30.

[9] McCormick CL, Salazar LC. J Macromol Sci, Pure Appl. Chem. 1992;A29:193–205.

[10] Noda T, Hashidzume A, Morishima Y. Polymer 2001;42:9243–52.

[11] Noda T, Hashidzume A, Morishima Y. Langmuir 2001;17:5984–91.

[12] Sato Y, Hashidzume A, Morishima Y. Macromolecules 2001;34: 6121–30.

[13] Hu Y, Smith GL, Richardson MF, McCormick CL. Macromolecules 1997;30:3526–37.

[14] Hu Y, Armentrout RS, McCormick CL. Macromolecules 1997;30: 3538–46.

[15] Kramer MC, Welch CG, Steger JR, McCormick CL. Macromolecules 1995;28:5248–54.

[16] Morishima Y, Nomura S, Ikeda T, Seki M, Kamachi M. Macromolecules 1995;28:2874–81.

[17] Binana-Limbelé W, Zana R. Macromolecules 1987;20:1331–5.

[18] Binana-Limbelé W, Zana R. Macromolecules 1990;23:2731–9.

[19] Yamamoto H, Tomatsu I, Hashidzume A, Morishima Y. Macromolecules 2000;33:7852–61.

[20] Suwa M, Hashidzume A, Morishima Y, Nakato T, Tomida M. Macromolecules 2000;33:7884–92.

[21] Chang Y, McCormick CL. Macromolecules 1993;26:6121–6.

[22] Branham KD, Snowden HS, McCormick CL. Macromolecules 1996; 29:254–62.

[23] Yamamoto H, Mizusaki M, Yoda K, Morishima Y. Macromolecules 1998;31:3588–94.

[24] Yamamoto H, Morishima Y. Macromolecules 1999;32:7469–75.

[25] Yusa S, Kamachi M, Morishima Y. Langmuir 1998;14:6059–67.

[26] Noda T, Morishima Y. Macromolecules 1999;32:4631–40.

[27] Noda T, Hashidzume A, Morishima Y. Macromolecules 2000;33: 3694–704.

[28] Noda T, Hashidzume A, Morishima Y. Langmuir 2000;16:5324–32.

[29] Noda T, Hashidzume A, Morishima Y. Macromolecules 2001;34: 1308–17.

[30] Morishima Y. In: Webber SE, Tuzar D, Munk P, editors. Solvents and self-organization of polymers. NATO ASI Series, Ser. E, vol. 327. The Netherland: Kluwer Academic Publishers; 1996. p. 331–58.

[31] Kaneko M, Yamada A. Adv Polym Sci 1984;55:1–47.

[32] Bader H, Dorn K, Hupfer B, Ringsdorf H. Adv Polym Sci 1985;64: 1–62.

[33] Tieke B. Adv Polym Sci 1985;71:79–151.

[34] Ringsdorf H, Schlarb B, Venzmer J. Angew Chem, Int Ed Engl 1988; 27:113–58.

[35] Paleos C, Malliaris A. J Macromol Sci Rev 1988;C28:403–19.

[36] Laschewsky A. Adv Polym Sci 1995;124:1–86.

[37] Salamone JC, Israel SC, Taylor P, Snider B. Polymer 1973;14: 639–44.

[38] Salamone JC, Taylor P, Snider B, Israel SC. J Polym Sci, Polym Chem Ed 1975;13:161–70.

[39] Anton P, Laschewsky A. Makromol Chem, Rapid Commun 1991;12: 189–96.

[40] Köberle P, Laschewsky A, van den Boogaard D. Polymer 1992;33: 4029–39.

[41] Anton P, Laschewsky A. Makromol Chem 1993;194:601–24.

[42] Nagai K, Ohishi Y, Inaba H, Kudo S. J Polym Sci, Polym Chem Ed 1985;23:1221–30.

[43] Nagai K, Ohishi Y. J Polym Sci, Part A: Polym Chem 1987;25:1–14.

[44] Kramer MC, Steger JA, Hu Y, McCormick CL. Macromolecules 1996;29:1992–7.

[45] Cochin D, Candau F, Zana R. Macromolecules 1993;26:5755–64.

[46] Cochin D, Zana R, Candau F. Macromolecules 1993;26:5765–71.

[47] Cochin D, Zana A, Candau F. Polym Int 1993;30:491–8.

[48] Vaskova V, Renoux D, Bernard M, Selb J, Candau F. Polym Adv Technol 1995;6:441–51.

[49] Aoki S, Morimoto Y. Polym Bull 1996;37:777–84.

[50] Wilhelm M, Zhao C-L, Wang Y, Xu R, Winnik MA, Mura J-L, Riess G, Croucher MD. Macromolecules 1991;24:1033–40.

[51] Jakeš J. Czech J Phys 1988;B38:1305–16.

[52] Jakeš J, Štěpánek P. Czech J Phys 1990;40:972–83.

[53] Hill A, Candau F, Selb J. Macromolecules 1993;26:4521–32.

[54] Kulicke W-M, Kniewske R, Klein J. Prog Polym Sci 1982;8:373.

[55] van Os NM, Haak JR, Rupert LAM. Physico-chemical properties of selected anionic, cationic and nonionic surfactants. Amsterdam: Elsevier; 1993.

[56] Lumb MD, Weyl DA. J mol Spectrosc 1967;23:365–71.

[57] Todesco R, Van Bockstaele D, Gelan J, Martens H, Put J, De Schryver FC. J Org Chem 1983;48:4963–8.

[58] Turro NJ. Modern molecular photochemistry. Sausalito, CA: University Science; 1991.

[59] Perrin FCR. Hebd Seances Acad Sci 1924;178:1978–80.

[60] Hashimoto S, Thomas JK. J Am Chem Soc 1985;107:4655–62.

[61] Breymann U, Dreeskamp H, Koch E, Zander M, Fresenius' Z. Anal Chem 1978;293:208–10.